DOI: 10.1002/chem.200801310

Synthesis, Characterization, Cytotoxicity, and Hydrolytic Behavior of C_2- and C_1-Symmetrical Ti^{IV} Complexes of Tetradentate Diamine Bis(Phenolato) Ligands: A New Class of Antitumor Agents

Dani Peri, Sigalit Meker, Michal Shavit, and Edit Y. Tshuva*[a]

Abstract: We recently introduced a new class of bis(isopropoxo)–Ti^{IV} complexes with diamine bis(phenolato) ligands that possess antitumor activity against colon HT-29 and ovarian OVCAR-1 cells that is higher than that of the known Ti^{IV} compounds titanocene dichloride and budotitane as well as that of cisplatin. Herein, we elaborate on this family of compounds; we discuss the effect of structural parameters on the cytotoxic activity and hydrolytic behavior of these complexes, seeking a relationship between the two. Whereas complexes with small steric groups around the metal center possess high activity and lead mostly to formation of O-bridged polynuclear complexes with bound bis(phenolato) ligand upon water addition, bulky complexes hydrolyze to release all free ligands and are inactive. Slightly increasing the size of the N-donor substituents probably weakens the ligand binding in solution, and, thus, rapid hydrolysis is observed, leading to a lack of cytotoxicity, supporting the requirement for ligand inertness. Replacing the two isopropoxo ligands with a single catecholato unit gives a complex with a different geometry that exhibits slower hydrolysis and reduced cytotoxicity, suggesting some participation of labile ligand hydrolysis in the cytotoxicity mechanism. A crystallographically characterized O-bridged polynuclear species obtained from a biologically active bis(isopropoxo) complex upon water addition is inactive, which rules out its participation as the active species, yet suggests some role of the particular steric and electronic requirements allowing its formation in the activity mechanism. Additional measurements support rapid formation of the active species in the presence of cells prior to O-bridged Ti^{IV} cluster formation.

Keywords: antitumor agents · cytotoxicity · hydrolysis · phenolato ligands · titanium

Introduction

In the last two decades, much focus has been given to non-platinum transition-metal complexes that may exhibit cytotoxic properties in attempts to discover novel reagents of various reactivities and mechanisms that may lead to improved anticancer therapeutics.[1–13] The Ti^{IV} complexes titanocene dichloride ($[TiCl_2Cp_2]$, Cp = cyclopentadienide) and budotitane ($[Ti(bzac)_2(OEt)_2]$, bzac = benzoylacetonate, OEt = ethoxide) are two parent compounds (shown here) that possess promising antitumor activity against cisplatin-sensitive and -resistant cells; however, their hydrolytic instability inhibited their applicable use.[4–6,14–20] In the presence of water, the labile groups (Cl, OR; OR = alkoxide) are hydrolyzed first within seconds, followed by the hydrolysis of the more inert ligands (Cp, diketonato) within hours,[21] leading to unidentified aggregates that hamper further

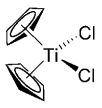

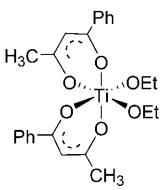

[a] D. Peri, S. Meker, M. Shavit, Dr. E. Y. Tshuva
Institute of Chemistry
The Hebrew University of Jerusalem, Jerusalem 91904 (Israel)
Fax: (+972) 2-658-4282
E-mail: tshuva@chem.ch.huji.ac.il

Supporting information for this article is available on the WWW under http://dx.doi.org/10.1002/chem.200801310. It contains color graphics for Figure 4–7, Figure 10–12, Figure 16, Figure 17; cytotoxicity measurements on OVCAR-1 cells, overlay of UV/Vis spectra upon water addition of $[Ti(L^n)(OiPr)_2]$ (n = 2–5), NMR spectra before and after D_2O addition of $[Ti(L^n)(OiPr)_2]$ (n = 2–4) and $[Ti(L^1)(O_2Ph)]$ at RT, NMR spectra for 14 h following D_2O addition at 37 °C for $[Ti(L^2)(OiPr)_2]$, NMR integration plots versus time for $[Ti(L^n)(OiPr)_2]$ (n = 2–4) at RT and/or at 37 °C, and spectroscopic data on $[Ti_3(L^1)_3(\mu_2\text{-}O)_3]$.

mechanistic investigations and ultimately lead to their failure in clinical trials. The nature of the active species, therefore, remains unknown, as does the identity of the biological target, the nature of the participation of the ligands, and the role of their particular lability.[20,22–25] Thus, the development of new Ti^{IV}-based cytotoxic compounds of defined hydrolytic behavior that may shed some light on this enigmatic process remains a significant challenge of immense value.

Another interesting observation is the interaction of titanocene dichloride with the serum protein transferrin.[26–31] This protein leads to complete ligand stripping from the Ti^{IV} core, and apparently allows somewhat selective cell penetration through the transferring receptors located more abundantly on tumor cell surfaces. Nevertheless, early loss of the most inert ligands abolishes their potential influence on the interaction with the biological target, and, thus, questions the contribution and influence of the particular ligand on the cytotoxic activity. Recent studies, however, suggested that potential binding of Ti^{IV} to albumin may also be achieved in the form of a ligand-bound complex,[32] which restores the interest in ligand design and structure–activity relationship studies by ligand modification, especially since labile complexes such as $[Ti(OiPr)_4]$ and $[TiCl_4(thf)_2]$ are biologically inactive.[23]

We have recently introduced a new family of cytotoxic agents based on readily accessible Ti^{IV} complexes of diamine bis(phenolato) ligands.[33] These complexes demonstrate some resemblance to the active budotitane in terms of covalent donor types, coordination number, and general symmetry; however, unlike budotitane, they are obtained quantitatively in a single step as single (racemic) isomers[17,34] and include a single tetradentate dianionic ligand instead of two monoanionic ones. Some members of this C_2-symmetrical family of complexes ($[Ti(L^n)(OiPr)_2]$ $n=1$ or 2) exhibit higher activity against colon HT-29 and ovarian OVCAR-1 cells than those measured for titanocene dichloride, budotitane, and cisplatin, which is independent of transferrin.[32] The reactivity is, however, strongly dependent on the particular ligand employed, since bulkier ligands ($[Ti(L^3)(OiPr)_2]$), aliphatic ligands, and ligands of branched donor connectivity that produce complexes of different symmetry all lead to substantially reduced activity.[33] Herein we elaborate on this family of complexes, discussing the effect of structural parameters on cytotoxicity and hydrolytic behavior of the complexes, while pointing to a connection between the two.

Results and Discussion

Ligand selection and complex preparation: In the current study, we were interested in evaluating the effect of structural parameters on the cytotoxic activity of this family of diamine–bis(phenolato) Ti^{IV} complexes and in gaining information on their hydrolytic behavior. Steric effects were examined by incorporating different substituents on the aromatic rings and N-donors. Particularly, the location of large steric groups may be of importance to elucidate whether their effect results from proximity to the metal and thus interferes with its interaction with various targets throughout hydrolysis or biological activity or from disruption to planarity which should preclude intercalation to DNA, a potential biological target, as has been suggested for budotitane.[17]

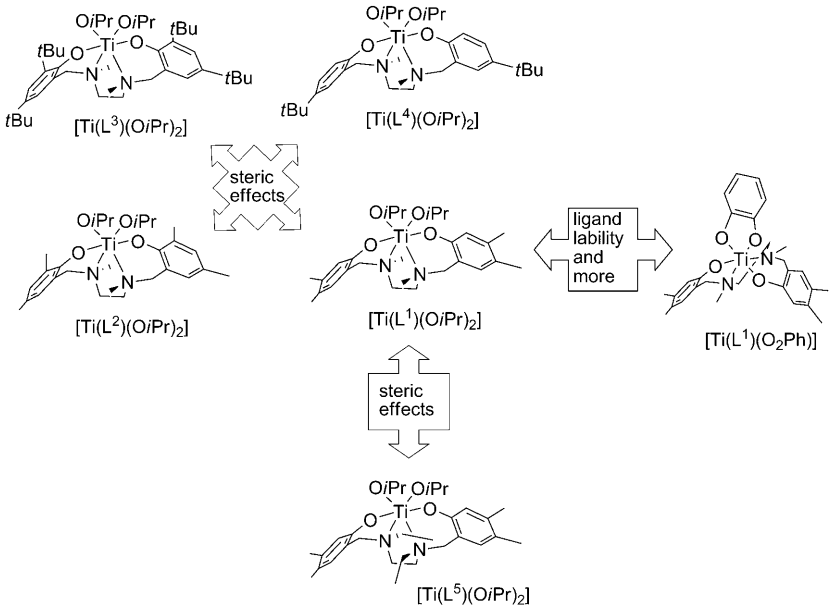

The complexes $[Ti(L^n)(OiPr)_2]$ ($n=1$–5) were prepared in quantitative yields according to a highly convenient, published procedure from the ligand precursors H_2L^n ($n=1$–5) and $[Ti(OiPr)_4]$ at room temperature in diethyl ether or THF.[33,35–37] The ligands were all synthesized by a single-step Mannich condensation from the substituted phenol, formaldehyde, and the *N*,*N*′-disubstituted diamine.[38] As we recently communicated,[33] the X-ray structure of $[Ti(L^1)(OiPr)_2]$ (Figure 1, top; Table 1) indicates a C_2-symmetrical complex with two *cis* isopropoxo groups and with the phenolato groups in a *trans* configuration, similar to other known compounds of this class.[36,37,39,40] Complex $[Ti(L^4)(OiPr)_2]$ was also crystallized from diethyl ether by slow evaporation at room temperature and the X-ray structure (Figure 2; Table 2) reveals a similar general geometry of a C_2-symmetrical complex with two *cis* isopropoxo groups and a *trans* configuration of the phenolato oxygen donors. Complex $[Ti(L^5)(OiPr)_2]$ was crystallized from diethyl ether at −35° C

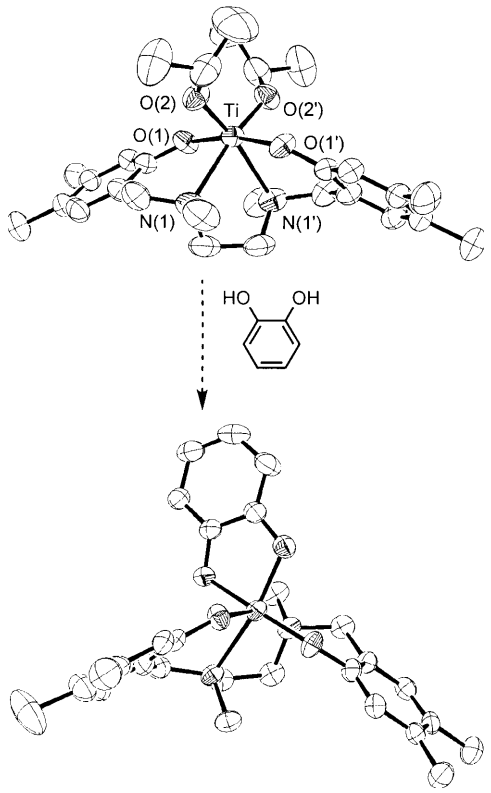

Figure 1. ORTEP drawing of $[Ti(L^1)(OiPr)_2]$ (top) and $[Ti(L^1)(O_2Ph)]$ (bottom) with 50% probability ellipsoids; H atoms omitted for clarity.

Table 1. Selected bond lengths [Å] and angles [°] for $[Ti(L^1)(OiPr)_2]$.

O(1)–Ti	1.9001(11)	N(1)–Ti	2.3449(16)
O(2)–Ti	1.8208(13)		
O(2)-Ti-O(2)	106.10(10)	O(1)-Ti-N(1)	88.61(5)
O(2)-Ti-O(1)	96.85(6)	O(1)-Ti-N(1)	81.22(5)
O(2)-Ti-O(1)	90.89(5)	O(2)-Ti-N(1)	163.37(7)
O(1)-Ti-O(1)	167.13(7)	O(2)-Ti-N(1)	89.44(6)
N(1)-Ti-N(1)	75.84(9)		

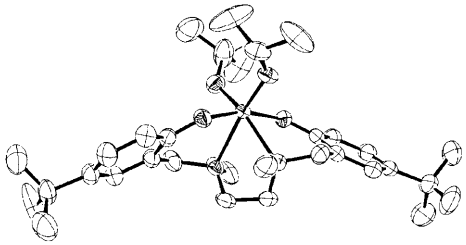

Figure 2. ORTEP drawing of $[Ti(L^4)(OiPr)_2]$ with 50% probability ellipsoids; H atoms omitted for clarity.

and its X-ray structure (Figure 3; Table 3) again shows a C_2-symmetrical complex with two *cis* isopropoxo groups and two *trans* phenolato donors, which is of very high structural similarity to its dimethyl analogue $[Ti(L^1)(OiPr)_2]$ (Figure 1, top), without any evidence for unusual steric tension. In particular, the Ti–N distances in $[Ti(L^5)(OiPr)_2]$ of 2.37–2.38 Å are only slightly longer than those observed for $[Ti(L^1)(OiPr)_2]$ (2.34 Å).[33] Thus, a very small influence of the extra methylene units on the complex structure and geometry is observed (Table 1, Table 3).

Table 2. Selected bond lengths [Å] and angles [°] for $[Ti(L^4)(OiPr)_2]$.

O(1)–Ti	1.900(2)	N(1)–Ti	2.312(3)
O(2)–Ti	1.905(2)	N(2)–Ti	2.360(3)
O(3)–Ti	1.820(2)		
O(4)–Ti	1.816(2)		
O(4)-Ti-O(3)	104.01(12)	O(4)-Ti-N(1)	164.88(12)
O(4)-Ti-O(1)	91.25(11)	O(3)-Ti-N(1)	89.92(12)
O(3)-Ti-O(1)	98.31(11)	O(1)-Ti-N(1)	80.79(10)
O(4)-Ti-O(2)	96.53(11)	O(2)-Ti-N(1)	88.36(10)
O(3)-Ti-O(2)	93.29(11)	O(4)-Ti-N(2)	90.40(11)
O(1)-Ti-O(2)	164.06(10)	O(3)-Ti-N(2)	164.94(11)
N(1)-Ti-N(2)	76.26(12)	O(1)-Ti-N(2)	85.52(10)
		O(2)-Ti-N(2)	80.55(10)

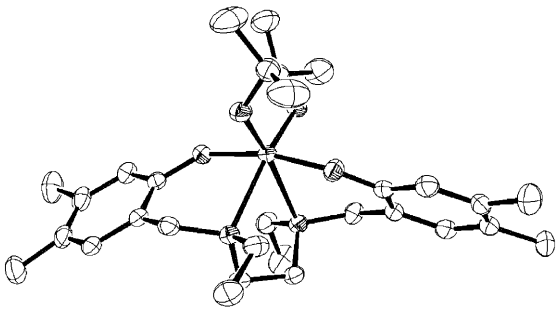

Figure 3. ORTEP drawing of $[Ti(L^5)(OiPr)_2]$ with 50% probability ellipsoids; H atoms omitted for clarity.

Table 3. Selected bond lengths [Å] and angles [°] for $[Ti(L^5)(OiPr)_2]$.

O(1)–Ti	1.904(2)	N(1)–Ti	2.369(2)
O(2)–Ti	1.898(2)	N(2)–Ti	2.376(2)
O(3)–Ti	1.835(2)		
O(4)–Ti	1.814(2)		
O(4)-Ti-O(3)	105.81(10)	O(4)-Ti-N(1)	163.49(9)
O(4)-Ti-O(1)	92.01(9)	O(3)-Ti-N(1)	90.28(9)
O(3)-Ti-O(1)	95.22(9)	O(1)-Ti-N(1)	82.68(8)
O(4)-Ti-O(2)	95.24(9)	O(2)-Ti-N(1)	87.58(9)
O(3)-Ti-O(2)	92.45(9)	O(4)-Ti-N(2)	88.91(9)
O(1)-Ti-O(2)	167.61(9)	O(3)-Ti-N(2)	164.24(9)
N(1)-Ti-N(2)	75.49(8)	O(1)-Ti-N(2)	89.71(8)
		O(2)-Ti-N(2)	80.41(8)

To evaluate the role of the lability of the O*i*Pr groups,[20,22–24] we also prepared the complex $[Ti(L^1)(O_2Ph)]$ (Ph = phenyl), which has one bidentate catecholato ligand instead of the two monodentate isopropoxo groups. This complex was synthesized by reacting $[Ti(L^1)(OiPr)_2]$ with one equivalent of *ortho*-catechol in THF at room temperature (Scheme 1). The ^1H NMR spectrum of the product revealed low symmetry, with four aromatic singlets of the bis(phenolato) ligand, four doublets of two AX systems of the ArCH_2 (Ar = aryl) groups, four doublets-of-triplets or mul-

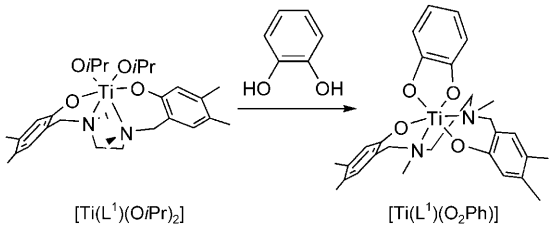

Scheme 1. Replacing two isopropoxo groups with a single catecholato unit.

tiplets of the NCH_2CH_2N bridge, four different Ar-CH_3 singlets, two different NMe signals, and two doublets-of-doublets and two doubles-of-triplets of the catecholato unit. Single crystals of [Ti(L^1)(O_2Ph)] suitable for X-ray crystallography were grown from diethyl ether at room temperature, and the ORTEP drawing of the structure is presented in Figure 1 (bottom). A list of selected bond lengths and angles is given in Table 4.

Table 4. Selected bond lengths [Å] and angles [°] for [Ti(L^1)(O_2Ph)].

O(1)–Ti	1.835(3)	N(1)–Ti	2.250(3)
O(2)–Ti	1.849(3)	N(2)–Ti	2.300(3)
O(3)–Ti	1.961(3)		
O(4)–Ti	1.909(3)		
O(4)-Ti-O(3)	81.05(12)	O(4)-Ti-N(1)	161.02(12)
O(4)-Ti-O(1)	107.61(12)	O(3)-Ti-N(1)	82.38(12)
O(3)-Ti-O(1)	94.45(12)	O(1)-Ti-N(1)	82.81(12)
O(4)-Ti-O(2)	97.86(13)	O(2)-Ti-N(1)	96.98(13)
O(3)-Ti-O(2)	170.58(12)	O(4)-Ti-N(2)	92.19(12)
O(1)-Ti-O(2)	94.79(12)	O(3)-Ti-N(2)	88.03(12)
N(1)-Ti-N(2)	78.04(12)	O(1)-Ti-N(2)	160.20(13)
		O(2)-Ti-N(2)	82.65(11)

Interestingly, the structure of [Ti(L^1)(O_2Ph)] features a compound of a different symmetry, namely C_1-symmetrical complex with the two phenolato groups of the tetradentate ligand in a *cis* configuration (Figure 1, bottom),[39] in contrast to the geometry of the starting complex (Figure 1, top). This result suggests an associative mechanism for ligand replacement, according to which a seven-coordinate intermediate is obtained upon the first nucleophilic attack on the metal center that causes ligand rearrangement, and a relatively rapid second attack to give the final product.

Cytotoxicity measurements and steric effects in [Ti(L^n)-(O*i*Pr)$_2$] (n=1–5): Cytotoxicity was measured on colon HT-29 and ovarian OVCAR-1 cells according to the MTT (methylthiazolyldiphenyltetrazolium bromide) assay.[33] The results obtained for [Ti(L^n)(O*i*Pr)$_2$] (n=1–3) in comparison to [$TiCl_2Cp_2$] after three days of incubation of the complexes with the cells with and without added apo-transferrin to the medium are summarized in Figure 4.[33] Substantial activity was observed for the complexes [Ti(L^n)(O*i*Pr)$_2$] (n=1 or 2), while no activity was observed for the bulky complex [Ti(L^3)(O*i*Pr)$_2$], indicating a major negative influence of the

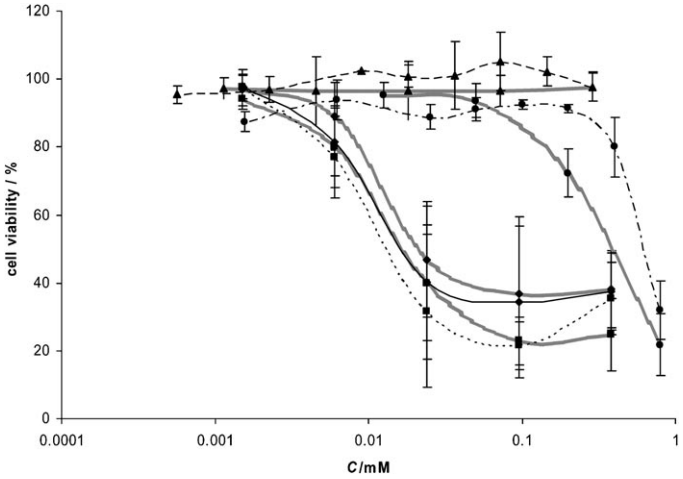

Figure 4. Dependence of HT-29 cell viability after 3 days of incubation on the concentration of [Ti(L^n)(O*i*Pr)$_2$] (n=1–3) and [$TiCl_2Cp_2$] administered presented in logarithmic scale with or without added apo-transferrin (10 μg mL^{-1}); see IC_{50} values in reference.[33] Thick solid curves: ▲: [Ti(L^3)(O*i*Pr)$_2$]+apo-transferrin; ◆: [Ti(L^2)(O*i*Pr)$_2$]+apo-transferrin; ■: [Ti(L^1)(O*i*Pr)$_2$]+apo-transferrin; ●: [$TiCl_2Cp_2$]+apo-transferrin; Other curves: ▲: [Ti(L^3)(O*i*Pr)$_2$]; ◆: [Ti(L^2)(O*i*Pr)$_2$]; ■: [Ti(L^1)(O*i*Pr)$_2$]; ●: [$TiCl_2Cp_2$].

large steric groups. It is also clear that the cell penetration mechanism for these complexes is independent of transferrin, unlike that of titanocene dichloride and similar to that of budotitane.[32] The dependence of the reactivity on the incubation time and the total loss of activity observed after exposing the complexes to the biological medium for two days prior to cell addition (Figure 5) suggest that the formed active species penetrates the cells quite rapidly through in a non-transferrin-dependent fashion, prior to complex dissociation and activity loss, and once in the cell the reactivity is retained.[33]

To evaluate the role of the particular location of the large *t*Bu (*t*Bu=*tert*-butyl) groups on abolishing activity, we studied the complex [Ti(L^4)(O*i*Pr)$_2$], which includes a single

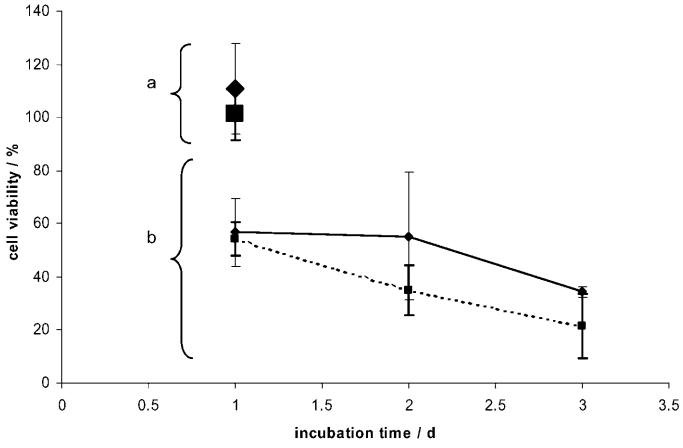

Figure 5. Dependence of HT-29 cell viability on incubation time a) with or b) without 2 days of exposure to the biological medium prior to cell administration of [Ti(L^n)(O*i*Pr)$_2$] (n=1 ■ and 2 ◆) at 0.1 mM.

bulky substituent that is rather distant from the metal site. Interestingly, some activity was observed towards HT-29 and OVCAR-1 cells, which is between that of $[Ti(L^1)(OiPr)_2]$ and that of $[Ti(L^3)(OiPr)_2]$ (Figure 6). This result is consistent with the observation regarding the negative effect of steric groups on activity; it points to an influence of peripheral groups as well and does not rule out a possible role of DNA intercalation in the cytotoxic activity of these complexes, especially considering the similar activity of $[Ti(L^1)(OiPr)_2]$ and $[Ti(L^2)(OiPr)_2]$ (Figure 4).

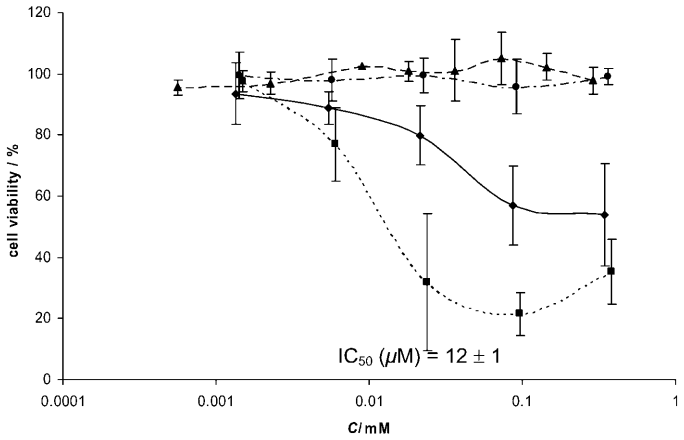

Figure 6. Dependence of HT-29 cell viability after 3 days of incubation on the concentration of $[Ti(L^n)(OiPr)_2]$ ($n=1$ and 3–5) administered presented in logarithmic scale. ■: $[Ti(L^1)(OiPr)_2]$; ▲: $[Ti(L^3)(OiPr)_2]$; ◆: $[Ti(L^4)(OiPr)_2]$; ●: $[Ti(L^5)(OiPr)_2]$.

Incorporating only slightly larger substituents on the N-donors had an even more drastic effect; $[Ti(L^5)(OiPr)_2]$ with ethyl substituents on the bound nitrogen atoms instead of methyl groups is completely inactive against both cell types analyzed (Figure 6), despite its highly similar X-ray structure to that of $[Ti(L^1)(OiPr)_2]$ (Figures 1 and 3). It appears that even a rather small increase of the substituent bulk, when employed directly on the donor to the metal, has a significant negative influence on activity. This suggests that either an approachable metal site or strong ligand binding are required for activity, as the Ti–N bonds have probably been weakened by the larger substituents, despite the rather similar bond distances observed in the solid-state structures, which may also be affected by crystal packing parameters.

Hydrolysis studies and steric effects in $[Ti(L^n)(OiPr)_2]$ ($n=$ 1–5): We investigated the hydrolytic behavior of the complexes by three methods. Changes in the UV/Vis absorption upon water addition, particularly of the ligand-to-metal charge transfer (LMCT) band of the bis(phenolato) ligand at $\lambda=320$–350 nm allowed the evaluation of general hydrolytic behavior and the possible identification of new compounds formed over time. NMR studies were valuable to determine the particular nature of the new compounds, if formed. In addition, attempts to intentionally synthesize partial hydrolysis products with O-bridging ligands in replacement of the O*i*Pr groups were also made by a reaction of the complexes with specific amounts of water and crystallization of the resulting product.

UV/Vis measurements: In a general procedure, a Ti^{IV} complex was dissolved in THF, and water was added to give a 1:9 water/THF solution. The absorbance was monitored overtime for several hours. Interestingly, a slight shift in the LMCT band to longer wavelengths was detected within several hours, for the biologically active complexes $[Ti(L^n)(OiPr)_2]$ ($n=1$, 2, and 4), which does not decay to zero (Figure 7), and may imply formation of a new species that includes a bound bis(phenolato) ligand under these conditions. No such shift was detected for the biologically inactive $[Ti(L^n)(OiPr)_2]$ ($n=3$ and 5), for which $[Ti(L^5)(OiPr)_2]$ demonstrated a significantly more rapid hydrolysis process with the LMCT band fully decaying within the first hour of water addition.

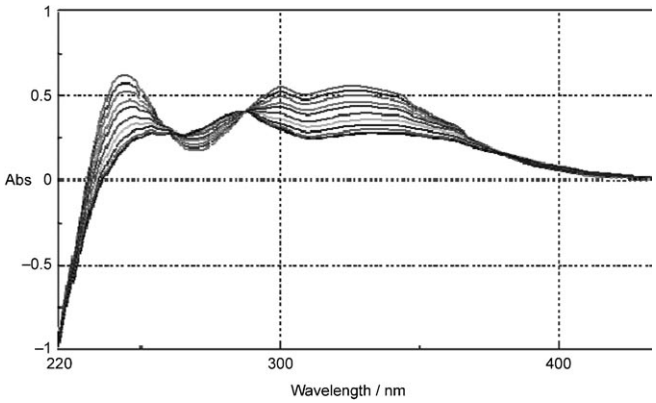

Figure 7. UV/Vis absorption over time for $[Ti(L^1)(OiPr)_2]$ upon addition of water to a solution of the complex in THF giving a 10% water solution.

As we suspected that exchange of the isopropoxo groups with water molecules giving O-bridged species should take place rapidly for all of these bis(isopropoxo) complexes,[1,14,21] we used a stopped flow instrument to identify possible quick changes within the first few seconds of water addition for $[Ti(L^n)(OiPr)_2]$ ($n=1$–3); no such changes were observed.

NMR measurements: To verify that no rapid hydrolysis reaction occurs within the first few minutes following water addition for $[Ti(L^n)(OiPr)_2]$ ($n=1$–4) and to gain information on the nature of the new species that may form within hours in some cases, as suggested by the UV-vis measurements, we added D_2O to a solution of the complexes in $[D_8]$THF to give a 1:9 $D_2O/[D_8]$THF mixture and took a ^1H NMR measurement every 4–10 minutes for several hours. To our surprise, the first spectrum taken following D_2O addition did not reveal a rapid reaction, and no indication of substantial isopropanol formation was observed for $[Ti(L^n)(OiPr)_2]$ ($n=$ 1–4).[41a] Only after several hours did the isopropanol signals

began to appear (Figure 8). For $[Ti(L^5)(OiPr)_2]$, the isopropanol signals appeared much more rapidly, in the very first measurement following D_2O addition (Figure 9), consistent with the results obtained by UV/Vis spectroscopy. Interestingly, for the biologically active complexes $[Ti(L^n)(OiPr)_2]$ ($n=1$, 2, and 4), the signals representing the free ligands that appeared within the measurement period were quite small and accompanied by many additional new signals of some new species (Figure 8), which appeared more rapidly for $[Ti(L^n)(OiPr)_2]$ ($n=1$ and 4) with *ortho* H atoms than for $[Ti(L^2)(OiPr)_2]$ with *ortho* methyl substituents. In contrast, only signals representing isopropanol and the free ligand H_2L^3 were observed for the biologically inactive bulky complex $[Ti(L^3)(OiPr)_2]$. Complex $[Ti(L^5)(OiPr)_2]$, which demonstrates significantly more rapid hydrolysis than $[Ti(L^n)(OiPr)_2]$ ($n=1$–4), also leads mainly to free ligand H_2L^5 signals although some tiny additional signals may be detected (Figure 9). Plotting the integration of the Ti–OC*H*-$(CH_3)_2$ signal, the $(CH_3)_2CHOH$ signal, one signal of a bound bis(phenolato) ligand, and one signal of a free ligand[41b] versus time (Figures 10–12) revealed that, for all complexes, all of the originally bound isopropoxo ligands are accounted for in the isopropanol formed, and in addition, the decay of integration of the bound bis(phenolato) ligand signal occurred simultaneously with isopropanol formation. Looking closely at the results obtained for the biologically inactive complexes $[Ti(L^3)(OiPr)_2]$ and $[Ti(L^5)(OiPr)_2]$ reveals that the integration of the signals for free bis(phenolato) ligand increases over a similar timescale to that of isopropanol formation despite the expected difference in their lability (Figures 11 and 12);[41b] however, while for $[Ti(L^3)(OiPr)_2]$ all of the ligand was released and no additional signals appeared in the final spectrum (Figure 11), for $[Ti(L^5)(OiPr)_2]$, only ≈50% of the bound bis(phenolato) ligand can be accounted for (Figure 12). Although we could not clearly detect a gradual increase in integration for the new signals observed for $[Ti(L^5)(OiPr)_2]$, it is conceivable that some new species is obtained with lower symmetry, which is represented by the multiple, small, difficult-to-analyze signals. One distinctive feature in the hydrolytic behavior of $[Ti(L^3)(OiPr)_2]$ (Figure 11) is slower initial hydrolysis that becomes faster with time and is probably due to the release of tension following partial ligand dissociation. As all new signals observed for the biologically active complexes $[Ti(L^n)(OiPr)_2]$ ($n=1$ and 2) have quite small integration values, increasing the temperature of the NMR experiment to 37 °C was valuable to accelerate the reaction and observe its completion upon total decay of signals relating to the original complex and complete formation of the new species and free ligand (Figure 10). A similar timescale is observed for the two processes in which both complexes release ≈20% of the bis(phenolato) ligand as free ligand H_2L and the final complicated spectrum clearly reveals substantial

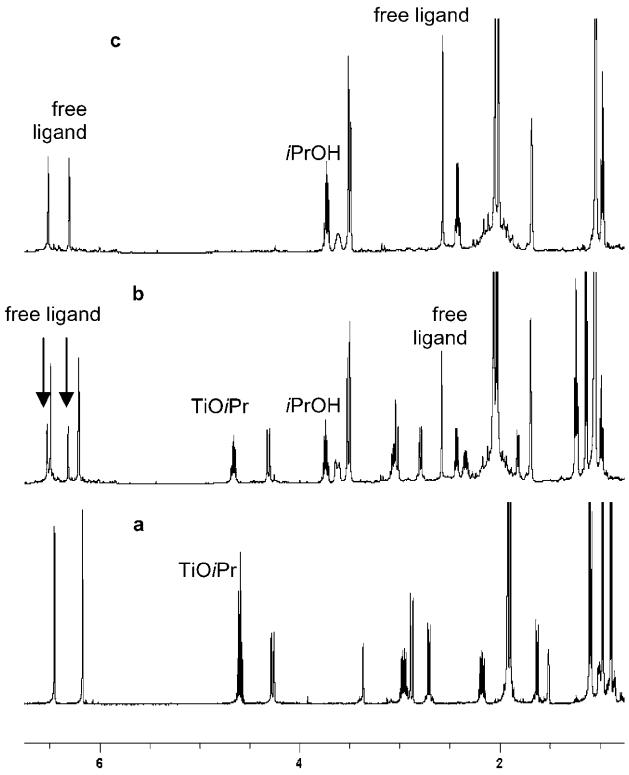

Figure 9. ^1H NMR spectra of $[Ti(L^5)(OiPr)_2]$ at RT a) in $[D_8]$THF, b) immediately following the addition of D_2O, and c) 1 h following the addition of D_2O.

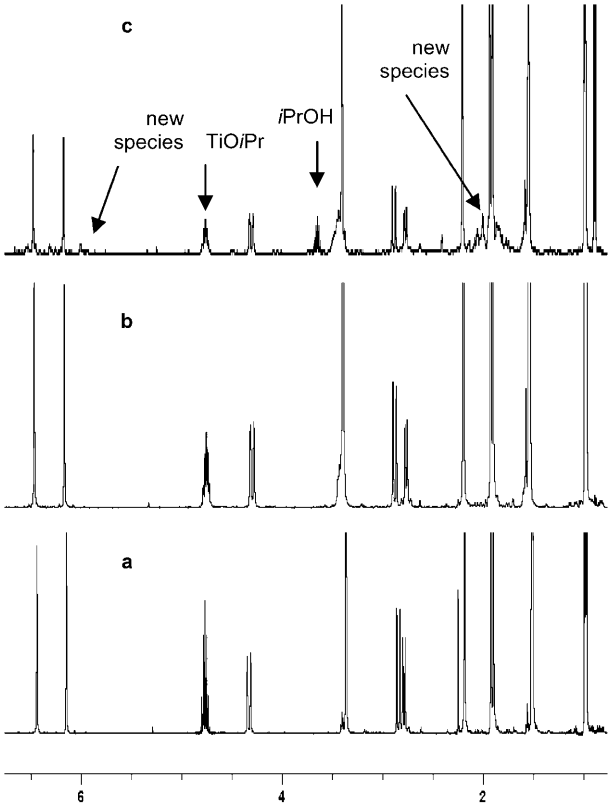

Figure 8. ^1H NMR spectra of $[Ti(L^1)(OiPr)_2]$ at RT a) in $[D_8]$THF, b) immediately following the addition of D_2O, and c) 3.5 h following the addition of D_2O.

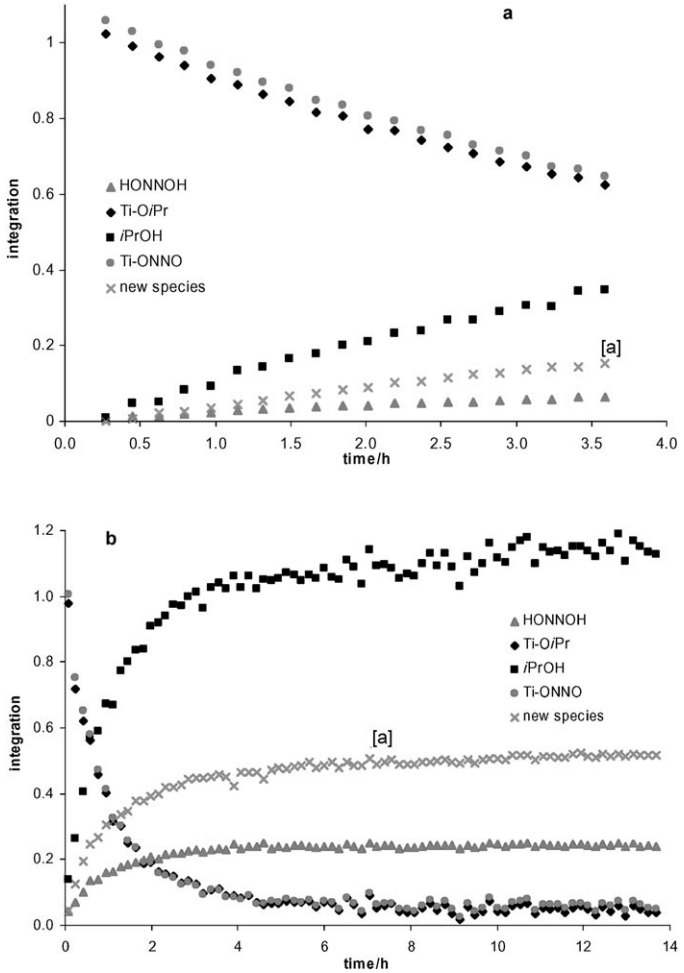

Figure 10. A plot of the integration of selected signals in the ^{1}H NMR spectrum of $[Ti(L^1)(OiPr)_2]$ versus time following addition of D_2O to a solution of the complex in $[D_8]$THF at a) RT and b) 37 °C; [a] The integration values for this particular plot of the "new species" were not calibrated like the rest[41b] due to the complexity of the spectrum and difficulty in assigning particular proton identity.

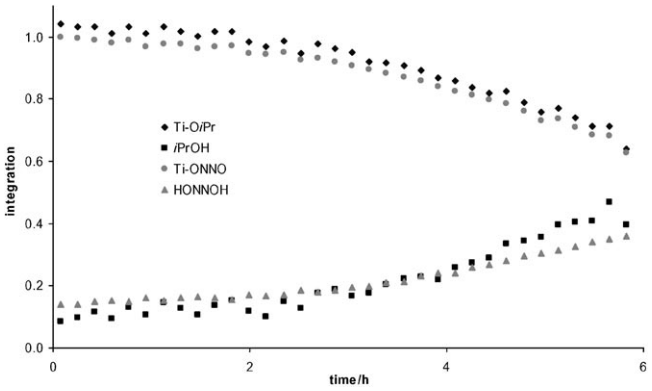

Figure 11. A plot of the integration of selected signals in the ^{1}H NMR spectrum of $[Ti(L^3)(OiPr)_2]$ versus time following the addition of D_2O to a solution of the complex in $[D_8]$THF at RT.

formation of a new compound (Figure 13). As the sum of the final integration of the free ligand and new species is

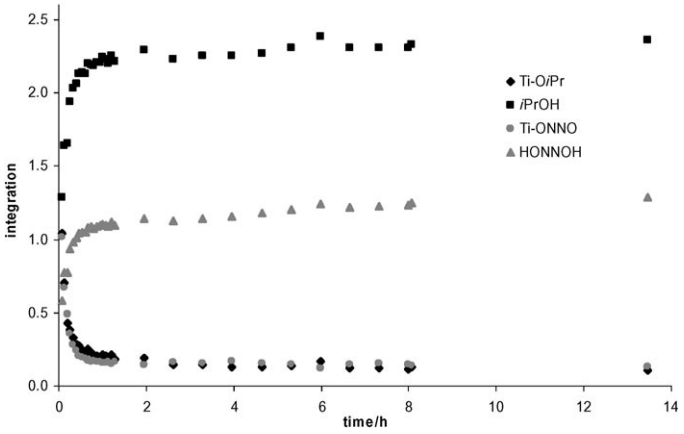

Figure 12. A plot of the integration of selected signals in the ^{1}H NMR spectrum of $[Ti(L^5)(OiPr)_2]$ versus time following the addition of D_2O to a solution of the complex in $[D_8]$THF at RT.

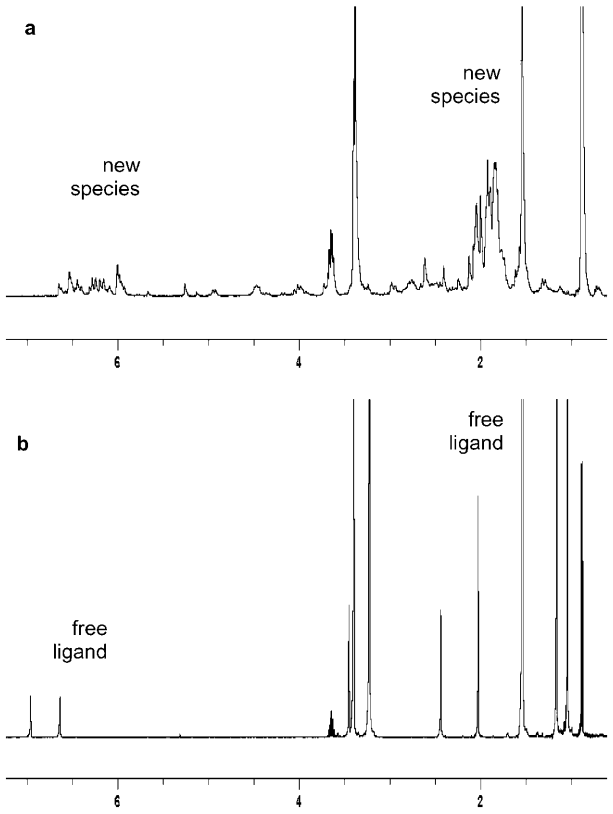

Figure 13. ^{1}H NMR spectrum of a) $[Ti(L^1)(OiPr)_2]$ and b) $[Ti(L^3)(OiPr)_2]$ in $[D_8]$THF 14 h following the addition of D_2O at 37 °C.

less than that of the starting complex, it is clear that the signal of the new species selected for the plot corresponds to a smaller number of protons, a fact that is also supported by its low symmetry as apparent by its multiple signals. As opposed to $[Ti(L^n)(OiPr)_2]$ ($n=1$ and 2), an experiment conducted with $[Ti(L^3)(OiPr)_2]$ at 37 °C supported complete ligand release to give only H_2L^3 and isopropanol (Figure 13).

To summarize, similar general hydrolytic behavior is observed for the two similarly active complexes $[Ti(L^n)(OiPr)_2]$ ($n=1$ and 2), namely, significant amount of new species formation relative to free bis(phenolato) ligand, with slower hydrolysis for the bulkier complex (Table 5). In contrast, the inactive complex $[Ti(L^3)(OiPr)_2]$ with bulkier *ortho*-substituents leads to complete free bis(phenolato) ligand release simultaneously with isopropanol release with no new species formation, while the inactive complex $[Ti(L^5)(OiPr)_2]$ with only slightly bulkier donor substituents relative to $[Ti(L^1)(OiPr)_2]$ demonstrates substantially faster hydrolysis (Table 5) with a smaller amount of new species formation. Complexes $[Ti(L^n)(OiPr)_2]$ ($n=1$ and 4) with similar *ortho* groups exhibit hydrolysis rates of the same order of magnitude despite the difference in cytotoxic activity, and $[Ti(L^n)(OiPr)_2]$ ($n=3$ and 5) , which are similarly inactive biologically, demonstrate significantly different rates of hydrolysis (Table 5). It is also quite surprising that in all processes in which a bis(phenolato) ligand is released, its hydrolysis rate is similar to that of the isopropoxo groups, which are hydrolyzed quite slowly for $[Ti(L^n)(OiPr)_2]$ ($n=1$–4).[42–46] Overall, these observations are consistent with those obtained by the UV/Vis measurements regarding formation of a new species in substantial amounts for the biologically active complexes $[Ti(L^n)(OiPr)_2]$ ($n=1$, 2, and 4).

Table 5. $t_{1/2}$ values for hydrolysis[a] of $[Ti(L^n)(OiPr)_2]$ ($n=1$–5) based on NMR measurements.

Complex	$t_{1/2}$	Complex	$t_{1/2}$
$[Ti(L^1)(OiPr)_2]$	5 h[b]	$[Ti(L^4)(OiPr)_2]$	3 h
$[Ti(L^2)(OiPr)_2]$	31 h[b]	$[Ti(L^5)(OiPr)_2]$	5 min
$[Ti(L^3)(OiPr)_2]$	10 h[b]		

[a] Hydrolysis rate calculated based on the release of Ti–O*i*Pr groups to give isopropanol. [b] Calculated based on trend-line.

Crystallographic measurements: The complex $[Ti(L^1)(OiPr)_2]$ was reacted with specific equivalents of water in an attempt to replace the isopropoxo groups and to produce O-bridged clusters with a bound diamine bis(phenolato) ligand, and perhaps gain structural information about the new species observed to form in the ^1H NMR measurements. Addition of one, two, or ten equivalents of water to a solution of $[Ti(L^1)(OiPr)_2]$ in THF and stirring at room temperature for three days gave a significant amount of single crystals that, somewhat surprisingly,[42–46] turned out to be the starting complex $[Ti(L^1)(OiPr)_2]$ (Figure 1, top). However, whereas increasing the amount of water to 100 equivalents gave similar results when the reaction was mixed for only 1.5 h, different single crystals suitable for X-ray crystallography were obtained in 95% yield when the reaction was allowed to stir with 50 equivalents of water for three days. Similar crystals were also obtained when the amount of water varied between 50 and 100000 equivalents. The structure of the product in all of these cases is presented in Figure 14 and selected bond lengths and angles are summarized in Table 6.

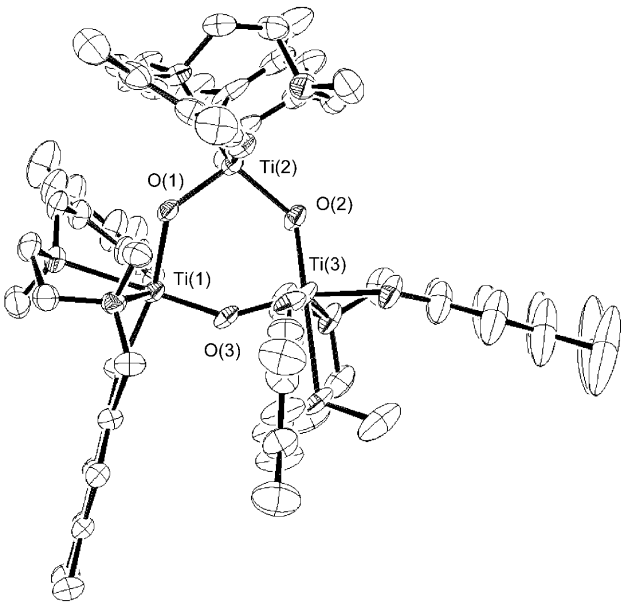

Figure 14. An ORTEP drawing of $[Ti_3(L^1)_3(\mu_2\text{-}O)_3]$ with 50% probability ellipsoids; H atoms and diethylether solvent were omitted for clarity.

Table 6. Selected bond lengths [Å] and angles [°] for $[Ti_3(L^1)_3(\mu_2\text{-}O)_3]$.

O(1)–Ti(2)	1.776(3)	O(8)–Ti(3)	1.864(3)
O(1)–Ti(1)	1.925(3)	O(9)–Ti(3)	1.905(3)
O(2)–Ti(3)	1.805(3)		
O(2)–Ti(2)	1.855(3)		
O(3)–Ti(1)	1.773(3)	N(1)–Ti(1)	2.369(4)
O(3)–Ti(3)	1.911(3)	N(2)–Ti(1)	2.293(4)
O(4)–Ti(1)	1.877(3)	N(3)–Ti(2)	2.414(4)
O(5)–Ti(1)	1.921(3)	N(4)–Ti(2)	2.361(4)
O(6)–Ti(2)	1.920(3)	N(5)–Ti(3)	2.387(4)
O(7)–Ti(2)	1.914(3)	N(6)–Ti(3)	2.284(4)
O(4)-Ti(1)-O(3)	104.07(12)	O(1)-Ti(2)-N(3)	167.33(13)
O(4)-Ti(1)-O(1)	96.24(13)	O(2)-Ti(2)-N(3)	88.45(13)
O(3)-Ti(1)-O(1)	95.37(13)	O(7)-Ti(2)-N(4)	78.02(12)
O(4)-Ti(1)-O(5)	92.86(13)	O(6)-Ti(2)-N(4)	88.81(12)
O(3)-Ti(1)-O(5)	95.88(14)	O(1)-Ti(2)-N(4)	94.20(13)
O(1)-Ti(1)-O(5)	163.37(13)	O(2)-Ti(2)-N(4)	160.50(14)
O(4)-Ti(1)-N(1)	80.92(13)	N(3)-Ti(2)-N(4)	74.31(13)
O(3)-Ti(1)-N(1)	175.01(13)	O(8)-Ti(3)-O(3)	93.85(13)
O(1)-Ti(1)-N(1)	83.90(12)	O(8)-Ti(3)-O(9)	93.02(14)
O(5)-Ti(1)-N(1)	83.84(14)	O(3)-Ti(3)-O(9)	164.30(13)
O(4)-Ti(1)-N(2)	157.54(13)	O(8)-Ti(3)-O(2)	107.75(13)
O(3)-Ti(1)-N(2)	98.04(13)	O(3)-Ti(3)-O(2)	94.06(13)
O(1)-Ti(1)-N(2)	85.44(12)	O(9)-Ti(3)-O(2)	97.26(15)
O(5)-Ti(1)-N(2)	80.90(13)	O(8)-Ti(3)-N(5)	83.84(13)
N(1)-Ti(1)-N(2)	76.99(13)	O(3)-Ti(3)-N(5)	81.94(13)
O(7)-Ti(2)-O(6)	162.29(13)	O(9)-Ti(3)-N(5)	84.78(15)
O(7)-Ti(2)-O(1)	98.18(13)	O(2)-Ti(3)-N(5)	168.04(13)
O(6)-Ti(2)-O(1)	94.52(13)	O(8)-Ti(3)-N(6)	160.07(14)
		O(3)-Ti(3)-N(6)	
O(7)-Ti(2)-O(2)	91.65(13)	O(9)-Ti(3)-N(6)	85.52(13)
O(6)-Ti(2)-O(2)	97.31(13)	O(2)-Ti(3)-N(6)	83.22(14)
O(1)-Ti(2)-O(2)	103.70(13)	N(6)-Ti(3)-N(5)	92.16(14)
O(7)-Ti(2)-N(3)	84.83(14)	O(1)-Ti(2)-N(3)	76.34(14)
O(6)-Ti(2)-N(3)	80.18(14)	O(2)-Ti(2)-N(3)	167.33(13)

The structure contains a trinuclear complex with three μ_2-O ligands. Interestingly, two out of the three Ti^{IV} centers

(Ti(1) and Ti(3)) feature *cis*-phenolato groups on the tetradentate ligand rather than a *trans* configuration as in the starting complex, and similar to the catecholato substituted product $[Ti(L^1)(O_2Ph)]$[39,47] (Figure 1, bottom), suggesting a similar mechanism for ligand replacement. A partial drawing that includes such a Ti^{IV} center and its bound ligands is presented in Figure 15. The Ti···Ti distances of the trinuclear

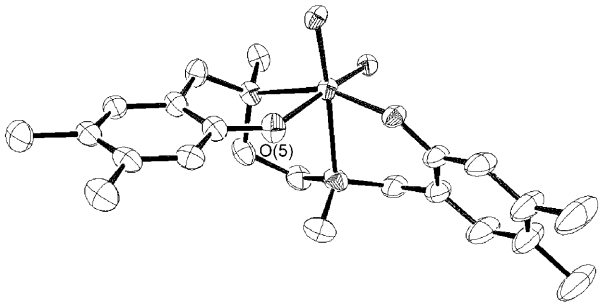

Figure 15. A partial ORTEP drawing of $[Ti_3(L^1)_3(\mu_2\text{-}O)_3]$ with 50% probability ellipsoids, which includes a single Ti^{IV} center.

core are in the range of 3.4–3.5 Å, with Ti–μ-O bond lengths of 1.77–1.93 Å and Ti-μ-O-Ti and μ-O-Ti-μ-O angles of 133.6–145.3° and 94.1–103.8°, respectively. Notably, the Ti^{IV} center of the *trans*-phenolato group exhibits a substantially wider μ-O-Ti-μ-O angle than that of the other two, as well as somewhat longer Ti–O and Ti–N bonds. Altogether, this structure exhibits a low symmetry of C_1, which explains the complicated NMR spectra obtained for the new species formed within several hours following water addition, and in particular, the integration ratio of the ligand signals (see above). Interestingly, the smallest distance between the two aromatic carbon atoms *ortho* to the phenolato oxygen atoms of two different bis(phenolato) ligands is 3.7 Å, with the distance between their corresponding hydrogen atoms being 3.3 Å. It is, therefore, logical that the *ortho*-methyl substituted analogue might be able to give an analogous structure through longer reaction times (Table 5), while an *ortho-tert*-butyl substituted analogue of this particular constrained structure is inconceivable. The ^{1}H NMR spectrum and LMCT absorption of the trinuclear complex are similar to those of the new species formed as described above. Therefore, if steric crowding allows, a new polynuclear species may form upon replacement of the isopropoxo groups; however, this process is not rapid for this family of complexes.[42–46]

Effect of ligand lability in $[Ti(L^1)(O_2Ph)]$: Replacing the two labile O*i*Pr groups with a single bidentate ligand in $[Ti(L^1)(O_2Ph)]$ gave a complex of enhanced hydrolytic stability as expected. Since the LMCT band of the bis(phenolato) ligand overlaps with that of the catecholato unit, analysis by UV/Vis is problematic. The ^{1}H NMR measured over time upon D_2O addition to a solution of $[Ti(L^1)(O_2Ph)]$ in $[D_8]$THF indicated partial hydrolysis in the formation of free catechol and free ligand H_2L^1 of around 10%, with no new signals that could be clearly detected (Figure 16). Since following the hypothetical hydrolysis of the catecholato

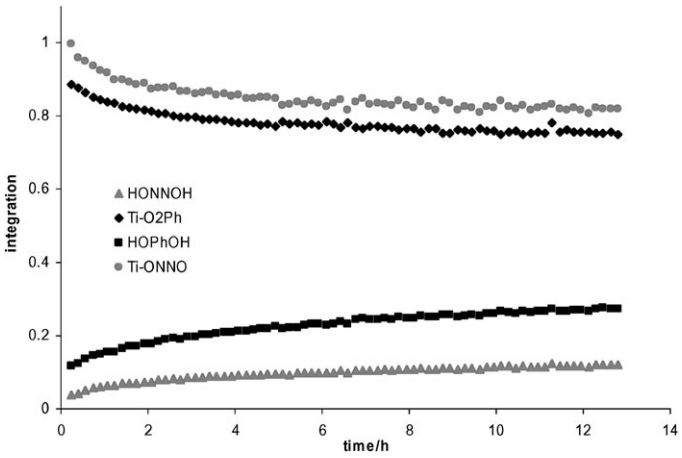

Figure 16. A plot of the integration of selected signals in the ^{1}H NMR spectrum of $[Ti(L^1)(O_2Ph)]$ versus time following the addition of D_2O to a solution of the complex in $[D_8]$THF at RT.

ligand the same L^1 ligand and its particular steric requirements remain as in $[Ti(L^1)(OiPr)_2]$, which is able to form a trinuclear complex, it is plausible that the strong binding of the catecholato ligand and perhaps also the different symmetry of the original complex prohibit this interaction, as the complex symmetry was previously observed to have a strong influence on activity.[33] Interestingly, this more inert complex also exhibits reduced cytotoxicity against both HT-29 and OVCAR-1 cells relative to $[Ti(L^1)(OiPr)_2]$ (Figure 17).[23] This observation supports the notion that the ligand steric requirements allow for some activity, yet some release of the labile groups needs to take place in order for

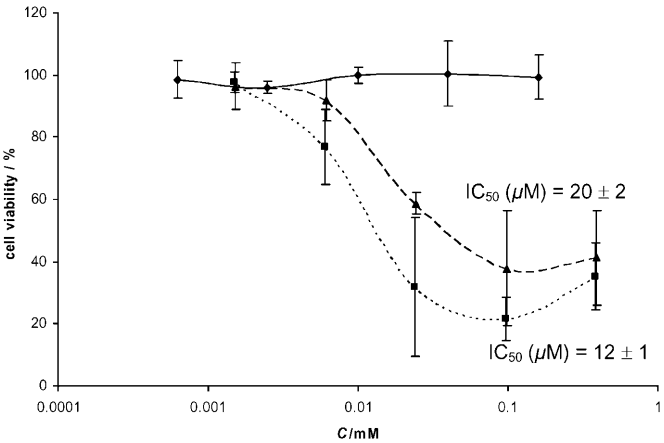

Figure 17. Dependence of HT-29 cell viability after 3 days of incubation on concentration of $[Ti(L^1)(OiPr)_2]$, $[Ti(L^1)(O_2Ph)]$, and $[Ti_3(L^1)_3(\mu_2\text{-}O)_3]$ administered presented in logarithmic scale. ◆: $[Ti_3(L^1)_3(\mu_2\text{-}O)_3]$; ▲: $[Ti(L^1)(O_2Ph)]$; ■: $[Ti(L^1)(OiPr)_2]$.

the complex to demonstrate activity. Perhaps, following this release, the symmetry of the original complex, namely the initial geometry of the ligand binding, is of lesser importance, as rearrangement could occur. This behavior is in general different from that observed with titanocene dichloride and its analogues, in which replacement of two chloride ligands with a bidentate oxalate significantly enhanced activity.[48]

What is the active species? As the active complexes $[Ti(L^n)(OiPr)_2]$ ($n=1$, 2, and 4) showed indications for rather substantial formation of an O-bridged bis(phenolato) polynuclear species upon water addition, while the inactive complex $[Ti(L^3)(OiPr)_2]$ leads to complete bis(phenolato) ligand release, we were interested in exploring whether the polynuclear complexes might be the actual active species as suggested for budotitane derivatives,[18–20,49] despite the apparent formation of smaller amounts of a polynuclear cluster from the inactive $[Ti(L^5)(OiPr)_2]$ as well. $[Ti_3(L^1)_3(\mu_2\text{-}O)_3]$, which is itself stable for days in the presence of water, was found to be inactive against the colon and ovarian cells measured (Figure 17). Thus, the well-defined cluster is not the active species formed through the hydrolysis of $[Ti(L^1)(OiPr)_2]$. This observation explains the lack of activity observed for $[Ti(L^5)(OiPr)_2]$. We thus suspect that, if not the cluster itself, then perhaps an intermediate in its formation might lead to activity, and, in general, the characteristics that allow its formation in terms of steric requirement are essential, although not suffice, for obtaining cytotoxic activity for this family of compounds.

Conclusion

In this work, we presented several octahedral Ti^{IV} complexes of tetradentate diamine bis(phenolato) ligands and explored the influence of steric effects and lability of the ligands on their cytotoxicity and hydrolytic behavior. Bulky groups have a negative effect on cytotoxicity, not merely when located in close proximity to the metal site, but also when located on the ligand periphery, judging from the similar cytotoxic activity of $[Ti(L^1)(OiPr)_2]$ and $[Ti(L^2)(OiPr)_2]$ and lower activity of $[Ti(L^4)(OiPr)_2]$. As the ability to form a polynuclear species upon water addition correlates with notable cytotoxic activity for $[Ti(L^n)(OiPr)_2]$ ($n=1$–4), we suspect that as large substituents near the metal center block the approach of two ligand-bound metal centers required to form a cluster, they may also block other biological interactions valuable for activity. More distant bulky substituent may have a similar influence; however, they may also point to some involvement of DNA intercalation in the biological activity, for which high ligand planarity is required. However, these observations may also reflect the effect of other parameters, such as solubility and/or cell penetration rate. In contrast, the near-metal-site steric effects represent the biggest influence on the hydrolysis rate: rather similar $t_{1/2}$ values for hydrolysis are observed for $[Ti(L^n)(OiPr)_2]$ ($n=1$ and 4) despite their different cytotoxicity; $[Ti(L^2)(OiPr)_2]$ with larger *ortho*-substituents relative to $[Ti(L^1)(OiPr)_2]$ (Me versus H) demonstrates slower hydrolysis despite the similar cytotoxicity of the two, presumably due to slower polynuclear complex formation requiring the proximity of two metal centers, while $[Ti(L^3)(OiPr)_2]$ does not form such a species (Table 5). Additionally, increasing steric bulk directly on the donor to the metal has an immensely negative effect on the cytotoxicity. As larger substituents should inhibit hydrolysis for complexes with strong chelating ligand binding, the substantially more rapid hydrolysis observed for $[Ti(L^5)(OiPr)_2]$ points to weaker ligand binding in solution despite the similar Ti–N bonds observed in the solid-state structures of $[Ti(L^n)(OiPr)_2]$ ($n=1$ and 5), and, thus, the reduced cytotoxicity of $[Ti(L^5)(OiPr)_2]$ presumably results from rapid formation of unreactive aggregates, which emphasizes the importance of a strongly bound chelating ligand as supported by the inactivity of particularly labile complexes.[23] Thus, we may generalize and say that mostly bis(phenolato) ligand release (whether it comes from weaker ligand binding, and thus a hydrolytically instable complex, or from large steric groups) vs. substantial polynuclear complex formation upon water addition, is more significant in determining biological activity than the particular rate of hydrolysis. This is particularly demonstrated by the immense difference in $t_{1/2}$ values of hydrolysis for the two similarly inactive complexes, $[Ti(L^n)(OiPr)_2]$ ($n=3$ and 5) and that of the similarly active ones $[Ti(L^n)(OiPr)_2]$ ($n=1$ and 2). Thus, a combination of strong chelating ligand binding and reduced steric bulk all around is required for activity. Overall, it is evident that careful design of particular ligands is essential in obtaining cytotoxicity of Ti^{IV} complexes as the ligand features have an immense influence on the hydrolysis and biological activity, which are not unrelated, while TiO_2 and labile $[Ti(OiPr)_4]$ and $[TiCl_4(thf)_2]$ are all inactive.[23]

As discussed, the ability to form polynuclear species through release of isopropoxo ligands upon water addition might be an important factor in obtaining cytotoxic agents from this family of compounds. This process becomes significantly disfavored for the catecholato complex, which shows not only enhanced hydrolytic stability, but also reduced cytotoxicity relative to its bis(isopropoxo) counterpart with the same tetradentate ligand. Still, one should not forget that the general geometry and symmetry of the catecholato complex is different from those of its bis(isopropoxo) counterpart, a parameter that itself may have a crucial influence on activity as we previously reported.[33] Nevertheless, it is plausible that the cytotoxic activity for these particular complexes[23] requires release of some labile ligands, especially considering the activity mechanism of cisplatin that involves DNA binding through the positions of the chloro groups following their hydrolysis. Thus, a combination of some lability of the monodentate groups and relative inertness of the bis(phenolato) ligand (see above) are essential. In addition, since the trinuclear complex isolated from the hydrolysis reaction of an active complex is itself inactive, the ability to

form it may point to an original complex of steric requirements suitable for its interaction with the biological target that leads to its activity, an interaction that must occur quite rapidly considering the deactivation of the complex after long periods in medium. Additional UV/Vis experiments involving the addition of biological medium (RPMI-1640) rather than pure water to $[Ti(L^n)(OiPr)_2]$ ($n=1$–3) and $[Ti_3(L^1)_3(\mu_2\text{-}O)_3]$ revealed LMCT band decay without any shift in λ_{max} for all of these complexes within several hours. Thus, it seems as if the active species is only rapidly formed in the presence of cells where steric crowding and electronic features allow, and once Ti–O aggregates are formed and/or ligands are completely released, the biological reactivity is lost. Therefore, the distinctive characteristics of the family of complexes presented herein regarding mediocre rate of hydrolysis of their O*i*Pr groups is of particular merit for biological applications.

Experimental Section

Ligands and their bis(isopropoxo) Ti^{IV} complexes were synthesized according to published procedures.[35–38] Data on $[Ti(L^n)(OiPr)_2]$ ($n=1$–3) can be found elsewhere.[33,36,37,50] Paraformaldehyde (95%) was purchased from Fluka Chemica and formaldehyde 30–38% assay was purchased from Bio Lab Ltd. and used without further purification. *N*,*N*′-Diethylethylenediamine (96%) was purchased from Alfa-Aesar a Johnson Matthey Company and used without further purification. Pyrocatechol (99%), 4-*tert*-butylphenol (99%), 3,4-dimethylphenol (99%), and *N*,*N*′-dimethylethylenediamine (99%) were purchased from Sigma-Aldrich Chemical Company and used without further purification. Titanium tetra(isopropoxide) (97%) was purchased from Aldrich Chemical Company. $[TiCl_2Cp_2]$ for reference measurements was purchased from Arapahoe Chemicals. All solvents were distilled from K or K/benzophenone under nitrogen. All experiments requiring dry atmosphere were performed in a M. Braun dry-box or under nitrogen atmosphere using Schlenk techniques. NMR data were recorded using an AMX-300, 400 or 500 MHz Bruker spectrometer. $CDCl_3$ (99.8%) and D_2O (99.9%) were purchased from Sigma-Aldrich Chemical Company and used without further purification. $[D_8]$THF (99.5%) was purchased from D-Chem and used without further purification. Hydrolysis experiments followed by NMR spectroscopy were conducted with a mixture of 90% $[D_8]$THF and 10% D_2O, in which the analysis was performed every 4–10 minutes. UV/Vis spectra were recorded on a Jasco V-530 spectrophotometer for which solutions ($\approx$0.05 mM) of the complexes in 90% THF and 10% water were used for the hydrolysis studies. Experiments involving the addition of biological medium were performed with RPMI-1640 medium purchased from Sigma without glutamic acid and without phenol red. Stopped flow measurements were performed on a HiTech Scientific diode-array instrument under similar conditions. Hydrolysis reactions for identifying O-bridged polynuclear complexes were performed on solutions of the complex (1.8 mmol) in THF by adding 1, 2, 10, 50, 100, 1000, 10000 or 100000 equivalents of water. X-ray diffraction data were obtained with Bruker Smart Apex diffractometer, running the SMART software package.[51] After collection, the raw data frames were integrated by the SAINT software package.[52] The structures were solved and refined using the SHELXTL software package. [53] Elemental analyses were performed in the microanalytical laboratory in our institute. Cytotoxicity was measured on HT-29 colon and OVCAR-1 ovarian cells obtained from ATCC using the methylthiazolyldiphenyl-tetrazolium bromide (MTT) assay as previously described.[33] Most complexes demonstrate incomplete solubility when the highest concentration is applied. Two of the free ligands demonstrate some cytotoxic activity (H_2L^4, H_2L^5); however, since complexes that rapidly hydrolyze to release the free ligands ($[Ti(L^5)(OiPr)_2]$) in pure water are still unreactive under biological conditions, we conclude that the reactivity measured for their complexes in vitro does not result from hydrolyzed ligand.

Synthesis of H_2L^4: H_2L^4 was synthesized by mixing 4-*tert*-butylphenol (20.0 mmol) with paraformaldehyde (20.0 mmol) and *N*,*N*′-dimethylethylenediamine (10.0 mmol) in methanol and heating to 50°C for 3 days. The crude product was cooled, filtered, and washed with cold methanol to yield H_2L^4 in 37%. ^{1}H NMR (400 MHz, $CDCl_3$): $\delta=7.2$ (dd, $J=8.6$, 2.4 Hz, 2H; Ar), 6.9 (s, 2H; Ar), 6.8 (d, $J=8.6$ Hz, 2H; Ar), 3.7 (s, 4H; CH_2), 2.7 (s, 4H; CH_2), 2.3 (s, 6H; NMe), 1.3 ppm (s, 18H; *t*Bu); ^{13}C NMR (400 MHz; $CDCl_3$): $\delta=155.3$, 141.8, 125.6, 125.2, 120.8, 115.6, 62.2, 54.3, 41.8, 33.9, 31.6 ppm; elemental analysis calcd (%) for $C_{26}H_{40}N_2O_2$ (412.6): C 75.68, H 9.77, N 6.79; found: C 75.93, H 9.95, N 6.94.

Synthesis of H_2L^5: H_2L^5 was synthesized by heating 3,4-dimethylphenol (5.0 mmol) with formaldehyde (10.0 mmol) and *N*,*N*′-diethylethylenediamine (2.5 mmol) to reflux in methanol for 5 h. The crude product was cooled, filtered, and washed with cold methanol to yield H_2L^5 in 67%. ^{1}H NMR (300 MHz, $CDCl_3$): $\delta=6.7$ (s, 2H; Ar), 6.6 (s, 2H; Ar), 3.7 (s, 4H; CH_2), 2.7 (s, 4H; CH_2), 2.6 (q, $J=7.06$ Hz, 4H; CH_2CH_3), 2.2 (s, 6H; $ArCH_3$), 2.1 (s, 6H; $ArCH_3$), 1.0 ppm (t, $J=7.06$ Hz, 6H; CH_2CH_3); ^{13}C NMR (400 MHz; $CDCl_3$): $\delta=155.6$, 136.9, 129.5, 126.8, 118.8, 117.3, 57.5, 50.4, 47.4, 19.6, 18.7, 11.0 ppm; elemental analysis calcd (%) for $C_{24}H_{36}N_2O_2$ (384.6): C 74.96, H 9.44, N 7.28; found: C 74.70, H 9.56, N 7.09.

Synthesis of $[Ti(L^4)(OiPr)_2]$: $[Ti(L^4)(OiPr)_2]$ was synthesized by treating $[Ti(OiPr)_4]$ (0.2 mmol) with H_2L^4 (0.2 mmol) in THF (8 mL) for 2 h at RT under a nitrogen atmosphere to give a yellow product in a quantitative yield. Yellow single crystals were obtained from diethyl ether by slow evaporation at RT. ^{1}H NMR (400 MHz, $CDCl_3$): $\delta=7.2$ (ddd, $J=$ 8.4, 2.6, 0.6 Hz, 2H; Ar), 6.9 (d, $J=2.4$ Hz, 2H; Ar), 6.6 (d, $J=8.3$ Hz, 2H; Ar), 5.0 (sept, $J=6.1$ Hz, 2H; $CHCH_3$), 4.7 (d, $J=13.2$ Hz, 2H; CH_2), 3.1 (d, $J=13.4$ Hz, 2H; CH_2), 3.0 (d $J=9.3$, Hz, 2H; CH_2), 2.5 (s, 6H; NMe), 1.8 (d, $J=9.3$ Hz, 2H; CH_2), 1.3 (s, 18H; *t*Bu), 1.3 (d, $J=$ 6.2 Hz, 6H; $CHCH_3$), 1.3 ppm (d, $J=6.0$ Hz, 6H; $CHCH_3$); ^{13}C NMR (400 MHz, $CDCl_3$): $\delta=159.6$, 140.1, 126.0, 125.6, 123.8, 116.6, 77.6, 64.9, 51.8, 47.3, 33.9, 31.7, 26.0, 25.7 ppm; UV/Vis (THF): λ_{max} (ε) = 328 nm (17210 $M^{-1}cm^{-1}$); elemental analysis calcd (%) for $C_{32}H_{52}N_2O_4Ti$ (576.3): C 66.65, H 9.09, N 4.86; found: C 66.93, H 9.31, N 5.03.

Crystal data for $[Ti(L^4)(OiPr)_2]$: $C_{32}H_{52}N_2O_4Ti$, $M=576.66$, monoclinic, $a=9.6622(7)$, $b=27.033(2)$, $c=13.4165(9)$ Å, $\beta=106.378(1)°$, $V=$ 3362.2(4) Å^3, $T=223(1)$ K, space group $P2_1/c$, $Z=4$, $\mu(Mo_{K\alpha})=$ 0.289 mm^{-1}, 34755 reflections measured, 6593 unique ($R_{int}=0.0461$); $R(F^2)$ for $[I>2\sigma(I)]=0.0839$, *R*w for $[I>2\sigma(I)]=0.1860$.

Synthesis of $[Ti(L^5)(OiPr)_2]$: $[Ti(L^5)(OiPr)_2]$ was synthesized similarly as a yellow solid in quantitative yield by treating $[Ti(OiPr)_4]$ (0.2 mmol) with H_2L^5 (0.2 mmol) in THF (5 mL) for 2 h at RT. Yellow single crystals were obtained from diethyl ether at −35°C. ^{1}H NMR (400 MHz, $CDCl_3$): $\delta=6.7$ (s, 2H; Ar), 6.5 (s, 2H; Ar), 4.9 (m, $J=6.1$ Hz, 2H; $CH(CH_3)_2$), 4.5 (d, $J=13.3$ Hz, 2H; CH_2), 3.2 (dq, $J=13.7$, 7.0 Hz, 2H; CH_2), 3.1 (d, $J=13.3$ Hz, 2H; CH_2), 2.9 (d, $J=10.1$ Hz, 2H; CH_2), 2.4 (dq, $J=13.6$, 6.9 Hz, 2H; CH_2), 2.2 (s, 6H; CH_3), 2.1 (s, 6H; CH_3), 1.8 (d, $J=10.2$ Hz, 2H; CH_2), 1.3 (t, $J=7.2$ Hz, 6H; CH_2CH_3), 1.2 (d, $J=6.4$ Hz, 6H; $CH(CH_3)_2$), 1.1 ppm (d, $J=6.1$ Hz, 6H; $CH(CH_3)_2$); ^{13}C NMR (400 MHz, $CDCl_3$): $\delta=159.9$, 136.8, 130.6, 125.0, 121.7, 118.2, 77.5, 58.2, 51.3, 48.2, 26.0, 25.9, 19.6, 18.7, 8.81 ppm; UV/Vis (THF): λ_{max} (ε) = 320 nm (20790 $M^{-1}cm^{-1}$); elemental analysis calcd (%) for $C_{30}H_{48}N_2O_4Ti$ (548.6): C 65.68, H 8.82, N 5.11; found: C 65.64, H 9.03, N 4.94.

Crystal data for $[Ti(L^5)(OiPr)_2]$: $C_{30}H_{48}N_2O_4Ti$, $M=548.60$, monoclinic, $a=15.017(1)$, $b=13.260(1)$, $c=15.157(1)$ Å, $\beta=100.960(1°)$, $V=$ 2963.0(4) Å^3, $T=173(1)$ K, space group $P2_1/n$, $Z=4$, $\mu(Mo_{K\alpha})=$ 0.325 mm^{-1}, 30243 reflections measured, 5827 unique ($R_{int}=0.0485$); $R(F^2)$ for $[I>2\sigma(I)]=0.0712$, *R*w for $[I>2\sigma(I)]=0.1498$.

Synthesis of $[Ti(L^1)(O_2Ph)]$: $[Ti(L^1)(O_2Ph)]$ was synthesized quantitatively by treating $[Ti(L^1)(OiPr)_2]$ (0.2 mmol) with pyrocatechol (0.2 mmol) in THF for 4 h at RT and under a nitrogen atmosphere to give a dark red solution. Following evaporation of the solvent, red single crystals were obtained from diethylether at RT. ^{1}H NMR (400 MHz, $CDCl_3$): $\delta=6.9$ (s,

1H; Ar), 6.8 (s, 1H; Ar), 6.7 (s, 1H; Ar), 6.6 (dt, $J=7.6$, 1.6 Hz, 1H; Ar-cat), 6.5 (dt, $J=7.6$, 1.6 Hz, 1H; Ar-cat; cat = catecholato), 6.5 (s, 1H; Ar), 6.4 (dd, $J=7.6$, 1.6 Hz, 1H; Ar-cat), 6.2 (dd, $J=7.6$, 1.6 Hz, 1H; Ar-cat), 5.2 (d, $J=13.1$ Hz, 1H; $ArCH_2N$), 4.7 (d, $J=13.5$ Hz, 1H; $ArCH_2N$), 3.7 (dt, $J=13.4$, 3.4 Hz, 1H; NCH_2CH_2), 3.4 (d, $J=13.5$ Hz, 1H; $ArCH_2N$), 3.2 (d, $J=13.2$ Hz, 1H; $ArCH_2N$), 3.1 (dt, $J=13.6$, 2.8 Hz, 1H; NCH_2CH_2), 2.7 (s, 3H; NMe), 2.5 (dd, $J=12.8$, 1.8 Hz, 1H; NCH_2CH_2), 2.2 (m, 1H; NCH_2CH_2), 2.2 (s, 3H; NMe), 2.2 (s, 3H; ArMe), 2.2 (s, 3H; ArMe), 2.2 (s, 3H; ArMe), 2.1 ppm (s, 3H; ArMe); ^{13}C NMR (400 MHz, $CDCl_3$): $\delta=194.0$, 160.2, 159.6, 158.6, 158.5, 138.0, 137.2, 130.6, 129.6, 128.7, 127.4, 122.8, 120.6, 120.1, 117.7, 117.6, 112.5, 111.5, 63.9, 63.4, 57.6, 52.0, 49.0, 42.9, 19.6, 19.5, 18.9, 18.8 ppm; UV/Vis (THF): λ_{max} (ε) = 344 nm (14610 $M^{-1}cm^{-1}$); elemental analysis calcd (%) for $C_{28}H_{34}N_2O_4Ti$ (510.2): C 65.88, H 6.71, N 5.49; found: C 65.59, H 6.72, N 5.46.

Crystal data for [Ti(L^1)(O$_2$Ph)]: $C_{28}H_{34}N_2O_4Ti$, $M=510.47$, monoclinic, $a=7.9048(8)$, $b=19.278(2)$, $c=16.699(2)$ Å, $\beta=95.756(2)°$, $V=2531.9(4)$ Å^3, $T=295(1)$ K, space group $P2_1/c$, $Z=4$, $\mu(Mo_{K\alpha})=0.375$ mm^{-1}, 26519 reflections measured, 4979 unique ($R_{int}=0.0847$); $R(F^2)$ for $[I>2\sigma(I)]=0.0816$, Rw for $[I>2\sigma(I)]=0.1451$.

Synthesis of [Ti$_3$(L^1)$_3$(μ$_2$-O)$_3$]: $[Ti_3(L^1)_3(\mu_2\text{-}O)_3]$ was synthesized by treating a solution of $[Ti(L^1)(OiPr)_2]$ (0.2 mmol) in THF (30 mL) with 50 equivalents of water in THF (10 mL) at RT under a nitrogen atmosphere for 3 days. Recrystallization from diethylether gave yellow single crystals in 95% yield. UV/Vis (THF): λ_{max} (ε) = 336 nm (27990 $M^{-1}cm^{-1}$); elemental analysis calcd (%) for $C_{66}H_{90}N_6O_9Ti_3$ (1255.2): C 63.16,H 7.23, N 6.70; found: C 63.19, H 7.53, N 6.50.

Crystal data for [Ti$_3$(L^1)$_3$(μ$_2$-O)$_3$]: $C_{66}H_{90}N_6O_9Ti_3\cdot C_4H_{10}O$, $M=1329.26$, monoclinic, $a=13.4535(9)$, $b=32.001(2)$, $c=16.669(1)$ Å, $\beta=104.678(1)°$, $V=7775.2(9)$ Å^3, $T=173(1)$ K, space group $P2_1/c$, $Z=4$, $\mu(Mo_{K\alpha})=0.354$ mm^{-1}, 80097 reflections measured, 15239 unique ($R_{int}=0.0418$). $R(F^2)$ for $[I>2\sigma(I)]=0.0991$, Rw for $[I>2\sigma(I)]=0.2346$.

CCDC 692997 ($[Ti(L^4)(OiPr)_2]$), 692998 ($[Ti(L^5)(OiPr)_2]$), 692999 ($[Ti(L^1)(O_2Ph)]$), and 693000 ($[Ti_3(L^1)_3(\mu_2\text{-}O)_3]$) contains the supplementary crystallographic data for this paper. These data can be obtained free of charge from The Cambridge Crystallographic Data Centre via www.ccdc.cam.ac.uk/data_request/cif.

Acknowledgement

We thank Dr. Shmuel Cohen for solution of the X-ray structures. We also thank HU for funding.

[1] M. J. Clarke, F. Zhu, D. R. Frasca, *Chem. Rev.* **1999**, *99*, 2511–2534.
[2] F. Kratz, M. T. Schütte, *Cancer J.* **1998**, *11*, 176–182.
[3] P. Köpf-Maier, *Eur. J. Clin. Pharmacol.* **1994**, *47*, 1–16.
[4] P. Koepf-Maier, H. Köpf, *Chem. Rev.* **1987**, *87*, 1137–1152.
[5] C. V. Christodoulou, A. G. Eliopoulos, L. S. Young, L. Hodgkins, D. R. Ferry, D. J. Kerr, *Brit. J. Cancer* **1998**, *77*, 2088–2097.
[6] F. Caruso, M. Rossi, C. Pettinari, *Expert Opin. Ther. Pat.* **2001**, *11*, 969–979.
[7] B. Desoize, *Anticancer Res.* **2004**, *24*, 1529–1544.
[8] G. Xu, Y. B. Cui, K. Cui, S. H. Gou, *Huaxue Jinzhan* **2006**, *18*, 107–113.
[9] M. Galanski, V. B. Arion, M. A. Jakupec, B. K. Keppler, *Curr. Pharm. Des.* **2003**, *9*, 2078–2089.
[10] I. Ott, R. Gust, *Arch. Pharm. Chem. Life Sci.* **2007**, *340*, 117–126.
[11] N. Katsaros, A. Anagnostopoulou, *Crit. Rev. Oncol. Hematol.* **2002**, *42*, 297–308.
[12] A. M. Evangelou, *Crit. Rev. Oncol. Hematol.* **2002**, *42*, 249–265.
[13] I. Kostova, *Curr. Med. Chem.* **2006**, *13*, 1085–1107.
[14] E. Melendez, *Crit. Rev. Oncol. Hematol.* **2002**, *42*, 309.
[15] P. Köpf-Maier, H. Köpf, *Struct. Bonding* **1988**, *70*, 103–185.
[16] G. Kelter, N. J. Sweeney, K. Strohfeldt, H.-H. Fiebig, M. Tacke, *Anti-Cancer Drugs* **2005**, *16*, 1091–1098.
[17] B. K. Keppler, C. Friesen, H. G. Moritz, H. Vongerichten, E. Vogel, *Struct. Bonding* **1991**, *78*, 97–127.
[18] F. Caruso, M. Rossi, J. Tanski, R. Sartori, R. Sariego, S. Moya, S. Diez, E. Navarrete, A. Cingolani, F. Marchetti, C. Pettinari, *J. Med. Chem.* **2000**, *43*, 3665–3670.
[19] F. Caruso, M. Rossi, *Mini-Rev. Med. Chem.* **2004**, *4*, 49–60.
[20] F. Caruso, M. Rossi, C. Opazo, C. Pettinari, *Bioinorg. Chem. Appl.* **2005**, *3*, 317–329.
[21] J. H. Toney, T. J. Marks, *J. Am. Chem. Soc.* **1985**, *107*, 947–953.
[22] P. Yang, M. Guo, *Coord. Chem. Rev.* **1999**, *185*, 189–211.
[23] M. Shavit, D. Peri, A. Melman, E. Y. Tshuva, *J. Biol. Inorg. Chem.* **2007**, *12*, 825–830.
[24] M. Ravera, C. Cassino, E. Monti, M. Gariboldi, D. Osella, *J. Inorg. Biochem.* **2005**, *99*, 2264–2269.
[25] F. Caruso, L. Massa, A. Gindulyte, C. Pettinari, F. Marchetti, R. Pettinari, M. Ricciutelli, J. Costamagna, J. C. Canales, J. Tanski, M. Rossi, *Eur. J. Inorg. Chem.* **2003**, 3221–3232.
[26] S. H. Sun, H. Li, R. A. Weir, P. J. Sadler, *Angew. Chem.* **1998**, *110*, 1622–1625; *Angew. Chem. Int. Ed.* **1998**, *37*, 1577–1579.
[27] M. Guo, H. Sun, H. J. McArdle, L. Gambling, P. J. Sadler, *Biochemistry* **2000**, *39*, 10023–10033.
[28] M. Guo, H. Sun, S. Bihari, J. A. Parkinson, R. O. Gould, S. Parsons, P. J. Sadler, *Inorg. Chem.* **2000**, *39*, 206–215.
[29] L. M. Gao, R. Hernandez, J. Matta, E. Melendez, *J. Biol. Inorg. Chem.* **2007**, *12*, 959–967.
[30] A. D. Tinoco, C. D. Incarvito, A. M. Valentine, *J. Am. Chem. Soc.* **2007**, *129*, 3444–3454.
[31] A. D. Tinoco, A. M. Valentine, *J. Am. Chem. Soc.* **2005**, *127*, 11218–11219.
[32] A. D. Tinoco, E. V. Eames, A. M. Valentine, *J. Am. Chem. Soc.* **2008**, *130*, 2262–2270.
[33] M. Shavit, D. Peri, C. M. Manna, J. S. Alexander, E. Y. Tshuva, *J. Am. Chem. Soc.* **2007**, *129*, 12098–12099.
[34] E. Dubler, R. Buschmann, H. W. Schmalle, *J. Inorg. Biochem.* **2003**, *95*, 97–104.
[35] S. Gendler, S. Segal, I. Goldberg, Z. Goldschmidt, M. Kol, *Inorg. Chem.* **2006**, *45*, 4783–4790.
[36] C. A. J. Chmura, M. G. Davidson, M. D. Jones, M. D. Lunn, M. F. Mahon, A. F. Johnson, P. Khunkamchoo, S. L. Roberts, S. S. F. Wong, *Macromolecules* **2006**, *39*, 7250–7257.
[37] J. Balsells, P. J. Carroll, P. J. Walsh, *Inorg. Chem.* **2001**, *40*, 5568–5574.
[38] E. Y. Tshuva, N. Gendeziuk, M. Kol, *Tetrahedron Lett.* **2001**, *42*, 6405–6407.
[39] S. Groysman, E. Sergeeva, I. Goldberg, M. Kol, *Eur. J. Inorg. Chem.* **2005**, 2480–2485.
[40] A. Yeori, S. Groysman, I. Goldberg, M. Kol, *Inorg. Chem.* **2005**, *44*, 4466–4468.
[41] a) Some small changes in chemical shifts were observed following D_2O addition due to the different ratio of solvents. Evaporating the mixed solution and redissolving in pure $[D_8]$THF gave rise to an identical spectrum to that of the initial compound; b) the integration values were calibrated to represent the same number of protons.
[42] K. Matsumoto, Y. Sawada, B. Saito, K. Sakai, T. Katsuki, *Angew. Chem.* **2005**, *117*, 5015–5019; *Angew. Chem. Int. Ed.* **2005**, *44*, 4935–4939.
[43] D. Zhang, *Eur. J. Inorg. Chem.* **2007**, 4839–4845.
[44] T. Kemmitt, N. I. Al-Salim, G. J. Gainsford, *Inorg. Chem.* **2000**, *39*, 6067–6071.
[45] A. Kayan, D. Hoebbel, H. Schmidt, *J. Appl. Polym. Sci.* **2005**, *95*, 790–796.
[46] C. F. Campana, Y. Chen, V. W. Day, W. G. Klemperer, R. A. Sparks, *J. Chem. Soc. Dalton Trans.* **1996**, 691–702.
[47] G.-J. M. Meppelder, T. P. Spaniol, J. Okuda, *J. Organomet. Chem.* **2006**, *691*, 3206–3211.
[48] J. Claffey, M. Hogan, H. Müller-Bunz, C. Pampillon, M. Tacke, *ChemMedChem* **2008**, *3*, 729–731.

[49] F. Caruso, C. Pettinari, F. Marchetti, P. Natanti, C. Phillips, J. Tanski, M. Rossi, *Inorg. Chem.* **2007**, *46*, 7553–7560.
[50] S. Gendler, A. L. Zelikoff, J. Kopilov, I. Goldberg, M. Kol, *J. Am. Chem. Soc.* **2008**, *130*, 2144–2145.
[51] SMART-NT V5.6, Brucker AXS GmbH, Karlsruhe (Germany), **2002**.
[52] SAINT-NT V5.0, Brucker AXS GmbH, Karlsruhe (Germany), **2002**.
[53] SHELXTL-NT V6.1, Brucker AXS GmbH, Karlsruhe (Germany), **2002**.

Received: June 30, 2008
Revised: October 6, 2008
Published online: January 20, 2009

